Technical Memorandum

ITASCA Consulting Group, Inc.
an HCITASCA company

Date: **September 6, 2007**
To: **Tricia Hendren**
From: **David Potyondy**
Re: **Smooth-Joint Model Version 2 (for PFC2D/3D 4.0 manual)**

This document describes the Smooth-Joint Model Version 2, which is implemented in PFC2D/3D Version 4.0 Alpha 61 and above, and supported by fist 1-48 and above. This contact model is called udm_SmoothJoint, and its version number in the PFC executable is obtained using the PRINT MODEL command.

[Tricia: Please add this as Section 2.4.4 in the PFC2D/3D Theory and Background volume. Note that this document, in its entirety, will be identical in the 2D and 3D manuals.

Rename sections 2.4.4, 2.4.5 and 2.4.6 to 2.4.5, 2.4.6 and 2.4.7, respectively. Modify start of these three sections with something like: The model is implemented as a user-defined contact model with C++ source files of `X.cpp` and `X.h`, which are compiled into **udm_Y_{32,64}.dll**. The 32 and 64 suffixes indicate compatibility with the 32- or 64-bit executable, respectively.

Incorporate USING USER DEFINED CONTACT MODELS section from notes-UDM.txt into Section 2.4 Alternative Models.]

2.4.4 Smooth-Joint Model

The smooth-joint model simulates the behavior of an interface regardless of the local particle contact orientations along the interface. The behavior of a frictional or bonded joint can be modeled by assigning smooth-joint models to all contacts between particles that lie upon opposite sides of the joint. The model is implemented as a user-defined contact model with C++ source files of `SmoothJoint.cpp` and `SmoothJoint.h`. The model name is **udm_SmoothJoint**, and the property names are prefixed by **sj_**.

The smooth-joint model has the following properties.

- `sj_dip` and `sj_dd`: Dip angle (θ_p) and dip direction (θ_d) [degrees]
- `sj_kn` and `sj_ks`: Normal ($\bar{k}_n$) and shear ($\bar{k}_s$) stiffness per unit area [$\mathrm{N/m^3}$]
- `sj_rmul`: Radius multiplier ($\bar{\lambda}$) [-]

111 Third Avenue South • Suite 450 • Minneapolis, Minnesota 55401
Tel: (612) 371-4711 • icg@itascacg.com • www.hcitasca.com • Fax: (612) 371-4717

- `sj_fric`: Friction coefficient (μ) [-]
- `sj_da`: Dilation angle (ψ) [degrees]
- `sj_bmode`: Bond mode $\left(M = \left\{ \begin{array}{l} 0, \text{ not bonded \& never failed} \\ 1, \text{ not bonded \& failed in tension} \\ 2, \text{ not bonded \& failed in shear} \\ 3, \text{ bonded} \end{array} \right. \right)$ []
- `sj_bns`: Bond normal (tensile) strength (σ_c , $\sigma_c \geq 0$) [$\mathrm{N/m^2}$]
- `sj_bss`: Bond shear strength (τ_c , $\tau_c \geq 0$) [$\mathrm{N/m^2}$]

The following internal state variables of the smooth-joint model can also be accessed.

- `sj_xun`, `sj_yun`, `sj_zun`: Unit-normal vector ($\hat{\mathbf{n}}_\mathrm{j}$) defining the joint plane [m] (read-only)
- `sj_A`: Cross-sectional area (A) [$\mathrm{m^2}$] (read-only)
- `sj_Un`: Total normal displacement (U_n) [m] (read-write)
- `sj_xUs`, `sj_yUs`, `sj_zUs`: Total shear displacement ($\mathbf{U}_\mathrm{s}$) [m] (PFC2D uses first component only) (read-write)
- `sj_Fn`: Normal force (F_n) [N] (read-only)
- `sj_xFs`, `sj_yFs`, `sj_zFs`: Shear force ($\mathbf{F}_\mathrm{s}$) [N] (PFC2D uses first component only) (read-only)

2.4.4.1 Formulation

A typical smooth-joint contact is shown in Figure 1. The joint geometry consists of two initially coincident planar surfaces denoted as surface 1 and surface 2. The plane orientation is defined by the unit-normal vector $\hat{\mathbf{n}}_\mathrm{j}$, and surface 2 is defined such that $\hat{\mathbf{n}}_\mathrm{j}$ points into surface 2. The unit normal is defined by the dip angle (θ_p) in PFC2D and by the dip angle and dip direction (θ_d) in PFC3D using the same conventions as the PFC JSET command which are as follows:

$$\hat{\mathbf{n}}_\mathbf{j} = \begin{cases} \left(\sin\left(\theta_p\right), \cos\left(\theta_p\right)\right), & \text{PFC2D} \\ \left(\sin\left(\theta_p\right)\sin\left(\theta_d\right), \sin\left(\theta_p\right)\cos\left(\theta_d\right), \cos\left(\theta_p\right)\right), & \text{PFC3D} \end{cases} \tag{1}$$

Joint orientation is fixed w.r.t. the global axes, and thus, the joint does not rotate as the result of macroscopic rigid-body motion; if such motion occurs, then a mechanism to rotate the joint would need to be added. The contact will only be deleted if one of the contacting particles is deleted—i.e., it will not be deleted even if the contacting particles are no longer overlapping.

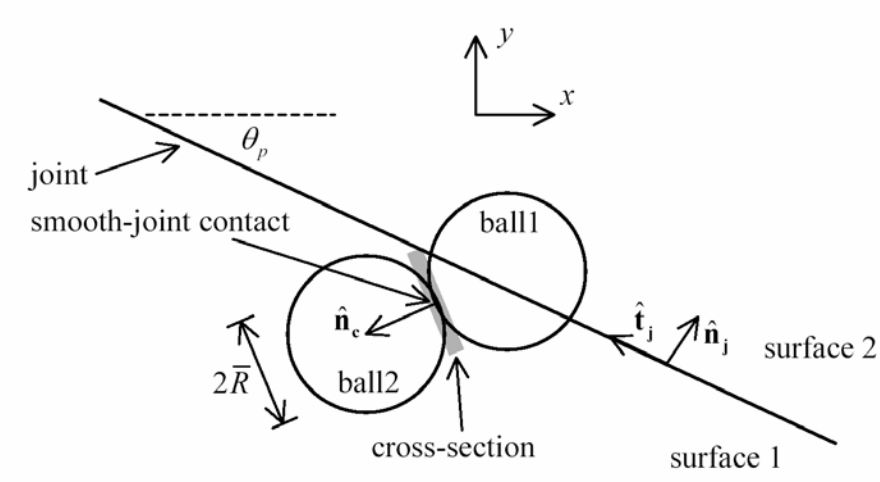

Figure 1 Notation used to define joint and smooth-joint contact

When the smooth-joint model is assigned to the contact, ball1 and ball2 are associated with the appropriate joint surfaces as follows. The contact unit-normal vector, $\hat{\mathbf{n}}_\mathbf{c}$, is directed from the center of ball1 to the center of ball2. The dot product of $\hat{\mathbf{n}}_\mathbf{c}$ and $\hat{\mathbf{n}}_\mathbf{j}$ is used to determine in which surface each ball lies such that ball2 lies in surface 2 iff $\hat{\mathbf{n}}_\mathbf{c} \cdot \hat{\mathbf{n}}_\mathbf{j} \geq 0$. The smooth joint can be envisioned as a set of elastic spring uniformly distributed over a rectangular cross section in PFC2D and a circular cross section in PFC3D lying on the joint plane and centered at the contact point. The area of the smooth-joint cross section is given by

$$A = \begin{cases} 2\bar{R}t, \quad t = 1, & \text{PFC2D} \\ \pi\bar{R}^2, & \text{PFC3D} \end{cases} \tag{2}$$

where smooth-joint radius $\bar{R} = \bar{\lambda} \min\left(R^{(A)}, R^{(B)}\right)$ with $R^{(A)}$ and $R^{(B)}$ being the particle radii. Let $\mathbf{U}$ be the translational displacement vector of surface 2 relative to surface 1, and let $\mathbf{F}$ be the force vector acting on surface 2. These vectors can be expressed as

$$\begin{aligned} \mathbf{U} &= U_n \hat{\mathbf{n}}_\mathbf{j} + \mathbf{U}_\mathbf{s} \\ \mathbf{F} &= F_n \hat{\mathbf{n}}_\mathbf{j} + \mathbf{F}_\mathbf{s} \end{aligned} \tag{3}$$

where $\mathbf{U}_\mathbf{s}$ and $\mathbf{F}_\mathbf{s}$ are the displacement and force vectors, respectively, that lie in the joint plane. Positive U_n denotes overlap, and positive F_n denotes compression. In PFC3D, the joint-plane vectors are stored explicitly, but in PFC2D, their magnitudes are stored and their values are obtained from

$$\begin{aligned} \mathbf{U}_\mathbf{s} &= U_s \hat{\mathbf{t}}_\mathbf{j} \\ \mathbf{F}_\mathbf{s} &= F_s \hat{\mathbf{t}}_\mathbf{j} \end{aligned} \tag{4}$$

where $\hat{\mathbf{t}}_\mathbf{j}$ is the unit-vector tangential to the joint plane that satisfies $\hat{\mathbf{n}}_\mathbf{j} \times \hat{\mathbf{t}}_\mathbf{j} = +\hat{\mathbf{k}}$ ($\hat{\mathbf{k}}$ points in the positive z-direction).

The contact force-displacement law provides either Coulomb sliding with dilation ($M < 3$) or bonded behavior ($M = 3$). When the smooth-joint model is assigned to the contact, the total force is set to zero and there is no bond ($M = 0$). A bond can be added by setting $M = 3$. During each subsequent time step, the relative translational displacement increment between the two ball surfaces is decomposed into components normal and tangential to the joint surfaces (ΔU_n and $\Delta \mathbf{U}_\mathbf{s}$). These components are multiplied by the smooth-joint normal and shear stiffnesses to produce increments of joint force. The total force is updated via

$$\begin{aligned} F_n &:= F_n + \bar{k}_n A \Delta U_n \\ \mathbf{F}_\mathbf{s}' &:= \mathbf{F}_\mathbf{s} + \bar{k}_s A \Delta \mathbf{U}_\mathbf{s} \end{aligned} \tag{5}$$

The joint is in one of two modes: unbonded ($M < 3$) or bonded ($M = 3$). The behavior differs for each mode as follows.

Unbonded joint (Figure 2)**:**

If $\left|\mathbf{F}_\mathbf{s}'\right| \le \left(F_s^* = \mu F_n\right)$, then $\left|\mathbf{F}_\mathbf{s}\right| = \left|\mathbf{F}_\mathbf{s}'\right|$; otherwise, sliding is assumed to occur and shear displacement during sliding produces an increase in normal force:

$$\left|\mathbf{F_s}\right| = F_s^*$$

$$F_n := F_n + \left[\Delta U_s^* \tan\psi\right]\bar{k}_n A = F_n + \left(\frac{\left|\mathbf{F_s}'\right| - F_s^*}{\bar{k}_s}\right)\bar{k}_n \tan\psi \tag{6}$$

where μ is the friction coefficient and ψ is the dilation angle.

Bonded joint (Figure 3)**:**

If $F_n \le -\sigma_c A$, then the bond breaks in tension ($M = 1$ and $F_n = \left|\mathbf{F_s}\right| = 0$); otherwise, the bond remains intact and F_n is not altered. If $\left|\mathbf{F_s}'\right| \ge \tau_c A$, then the bond breaks in shear ($M = 2$ and if the bond is in tension, then $F_n = \left|\mathbf{F_s}\right| = 0$; otherwise, F_n is not altered and $\left|\mathbf{F_s}\right| \le F_s^*$); otherwise, the bond remains intact and $\left|\mathbf{F_s}\right| = \left|\mathbf{F_s}'\right|$. In the above expressions, σ_c and τ_c are the bond normal and shear strengths, respectively, and *A* is the bond cross-sectional area.

The contact force is then mapped back into the local contact system and returned to the controlling PFC logic.

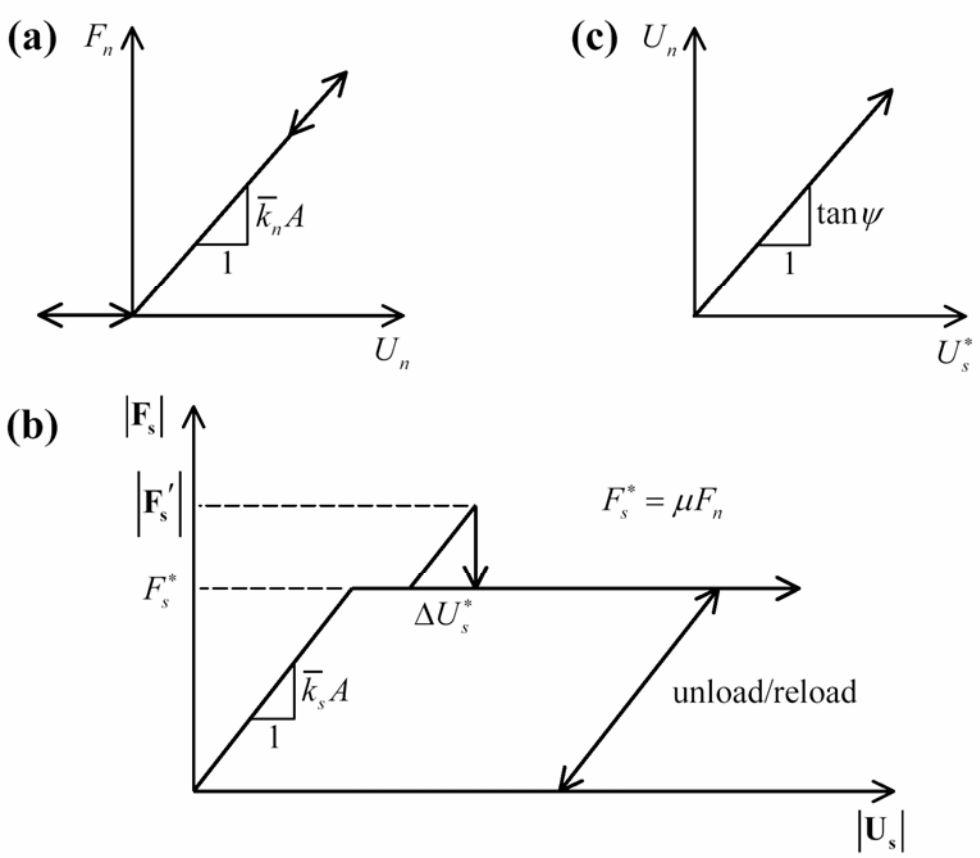

Figure 2 ***Force-displacement law for an unbonded joint: (a) normal force versus normal displacement, (b) shear force versus shear displacement and (c) normal displacement versus shear displacement during sliding***

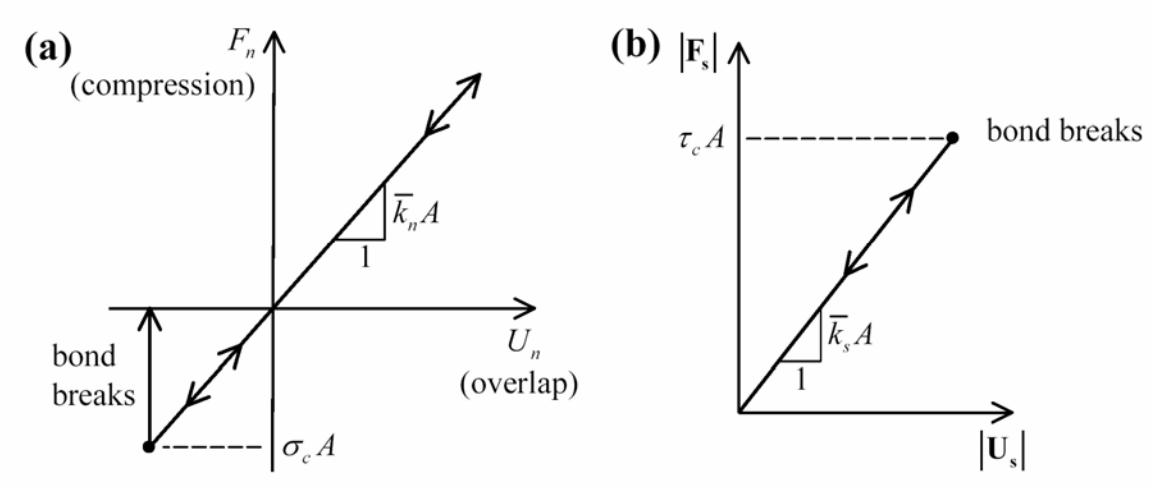

Figure 3 Force-displacement law for a bonded joint: (a) normal force versus normal displacement and (b) shear force versus shear displacement

2.4.4.2 Creating a single smooth-joint contact

This example (see data file `SmoothJoint{2d,3d}.dat`) demonstrates that the smooth-joint model operates correctly at a single contact. It shows how one can define a local planar surface with an orientation that does not coincide with the contact orientation. The model consists of two unit-radius particles oriented at 45-degrees from the $y = 0$ plane (see Figure 4). A smooth joint with unit normal aligned with the global y axis is assigned to the contact. It is assigned normal and shear stiffnesses of unity, a radius multiplier of one-half and a friction coefficient of zero. All degrees of freedom of both particles are fixed. The upper ball is first moved downward toward the $y = 0$ plane, and then moved parallel with the $y = 0$ plane. The normal and shear forces w.r.t. the joint plane are compressive ($F_n > 0$) and zero ($\mathbf{F}_s \cong 0$), respectively (see Figures 5 and 6). The friction coefficient is set to unity, and the upper ball continues to move parallel with the $y = 0$ plane. The change in normal force is negligible, and the shear-force magnitude now equals the normal force (see Figures 7 and 8).

[Add data files `SmoothJoint{2d,3d}.dat` here.]

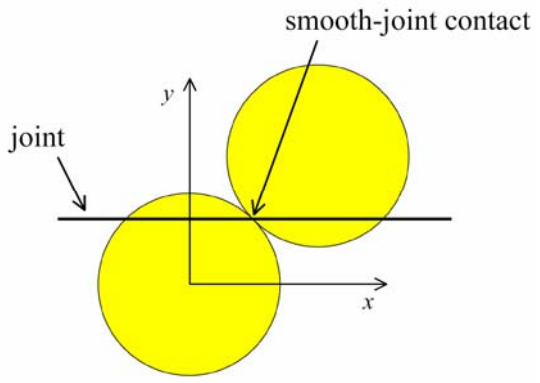

Figure 4 Initial system configuration

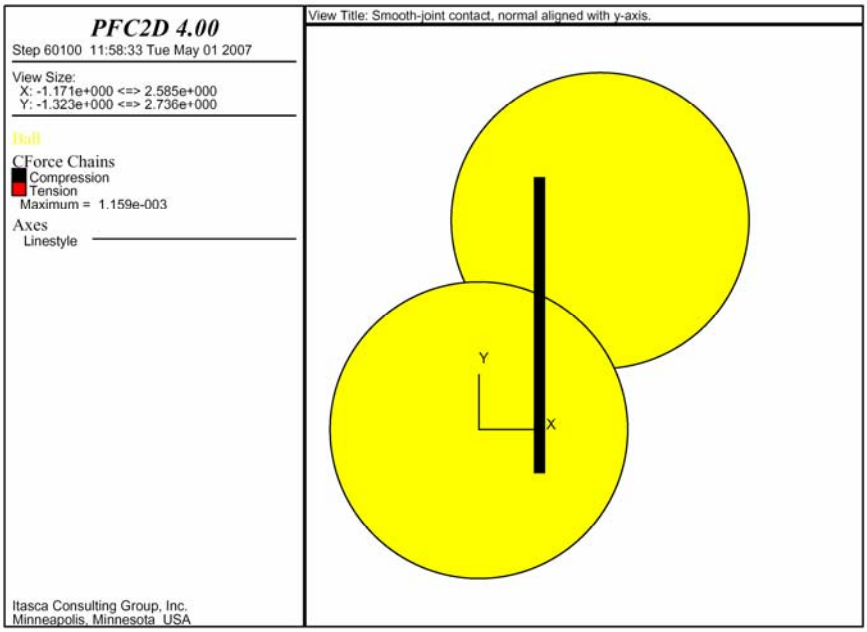

Figure 5 Contact force in PFC2D model after downward and left-horizontal motion of upper particle (friction coefficient of zero)

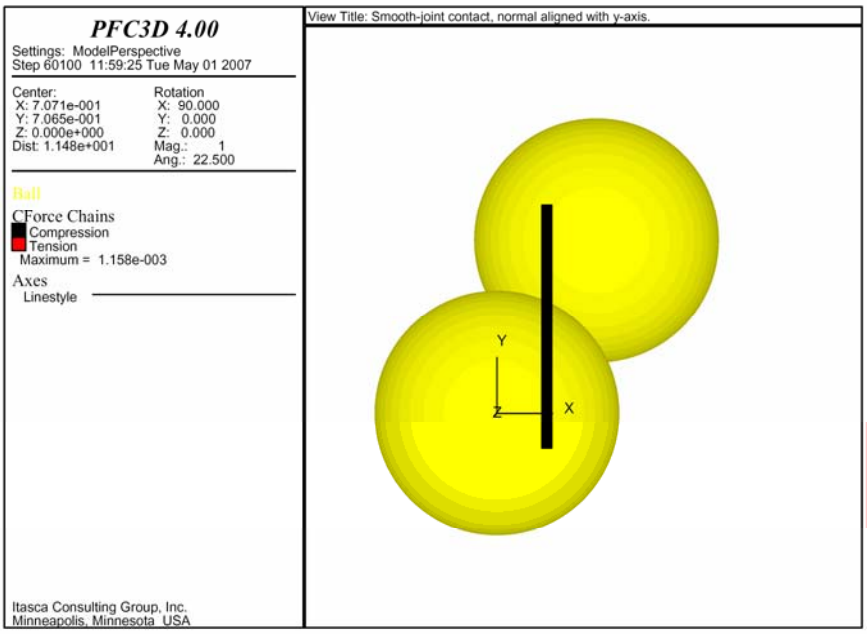

Figure 6 Contact force in PFC3D model after downward and left-horizontal motion of upper particle (friction coefficient of zero)

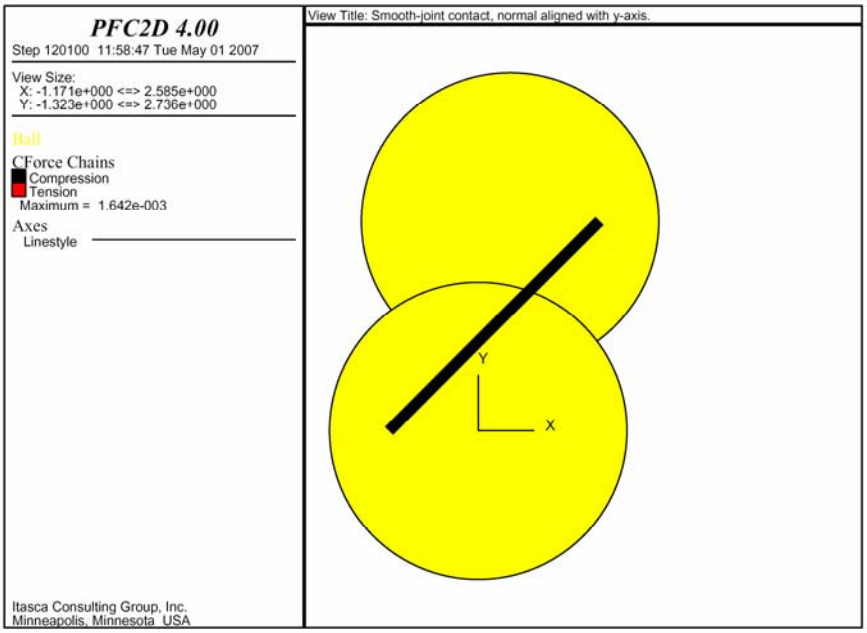

Figure 7 Contact force in PFC2D model after further left-horizontal motion of upper particle (friction coefficient of unity)

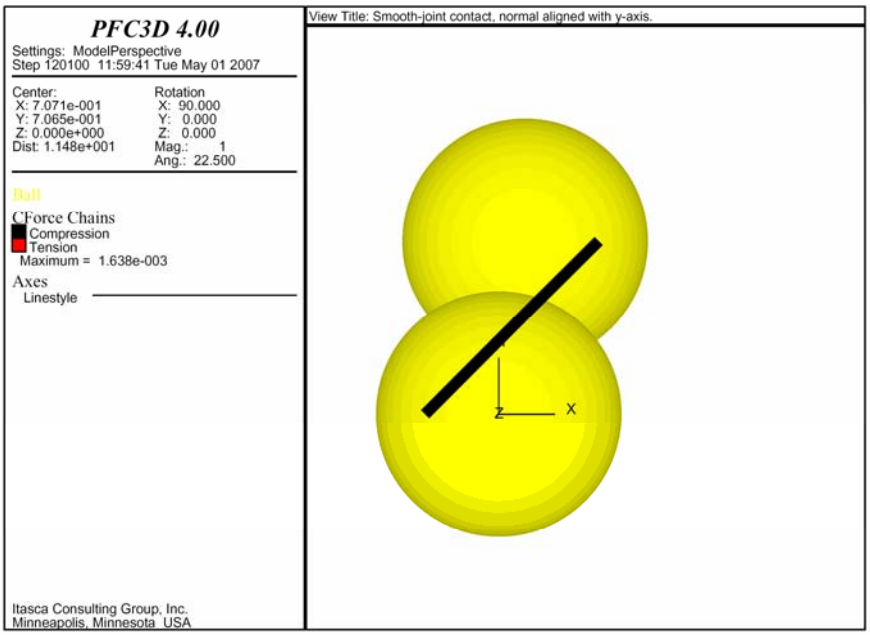

Figure 8 Contact force in PFC3D model after further left-horizontal motion of upper particle (friction coefficient of unity)

2.4.4.3 Modeling joints as collections of smooth-joint contacts

The PFC FishTank supports modeling joints as collections of smooth-joint contacts. A bonded-particle model is the starting point for the following procedure. A collection of zero-thickness disk-shaped joints and their properties are defined in two ASCII files that are read into the code by `jt_Read` such that joints are numbered sequentially starting from one. The function `sj_Make` creates a set of smooth-joint contacts by adding the joints one at a time, starting with the first joint. For each joint, contacts that satisfy the criterion of the **`c_ondisk()`** FISH intrinsic and do not already have a smooth-joint contact model are assigned a smooth-joint contact model with properties of the joint and a jset number equal to the joint number. If any parallel or contact bonds exist at these contacts, they are removed. The macroscopic joints can be visualized with the `jt_pi_geom` plot item, and the individual smooth-joint contacts can be visualized with the `sj_pi_geom` plot item. If large shearing displacements occur, then it may be necessary to trap new contacts that form near a joint and assign a smooth-joint contact model to them; otherwise, such new contacts will behave as interacting asperities because they will be assigned the default contact model and spurious contact forces will develop between them. Such asperity lockup can be prevented by setting the function `sj_Add` to be called whenever a new contact is created.

The first example (see the data files in the directories `fist\templates\LdB\2d\sj-2d` and `fist\templates\LdB\3d\sj-3d`, driven by `Solid1-sj.dvr`) adds a single through-going joint to a bonded-particle specimen, and then performs an unconfined-compression test on the specimen to demonstrate that the joint is behaving properly. A bonded-particle model of Lac du Bonnet granite with a resolution of approximately 10 particles across the specimen width is first created by setting `mg_Rmin=1.22e-3` in `..\..\resolution.dat`, and then calling `..\Solid-spc.dvr`. The 2D specimen is a square with side length of 30 mm, and the 3D specimen is a cylinder with height and diameter of 30 mm. In both the 2D and 3D models, the specimen axis is aligned with the global y axis. The 20-mm radius joint is placed at the center of the specimen and oriented with a –30 degree dip angle in the 2D model and a –60 degree dip angle and 0 degree dip direction in the 3D model. The joint is shown in Figures 9 and 10.

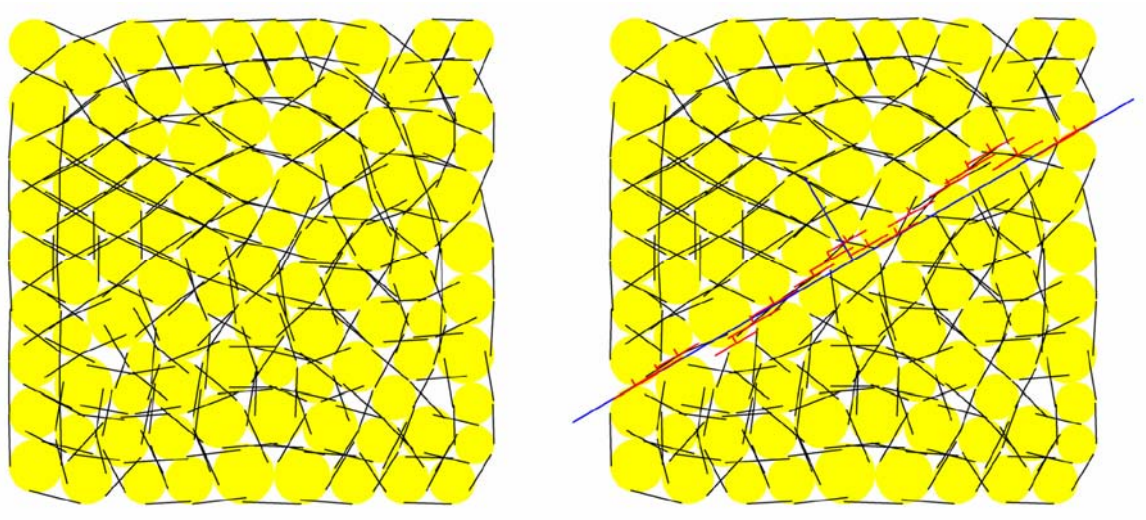

Figure 9 Particles, parallel bonds and joint in the PFC2D specimen (left: original specimen, right: specimen after insertion of smooth-joint contact models at 18 contacts)

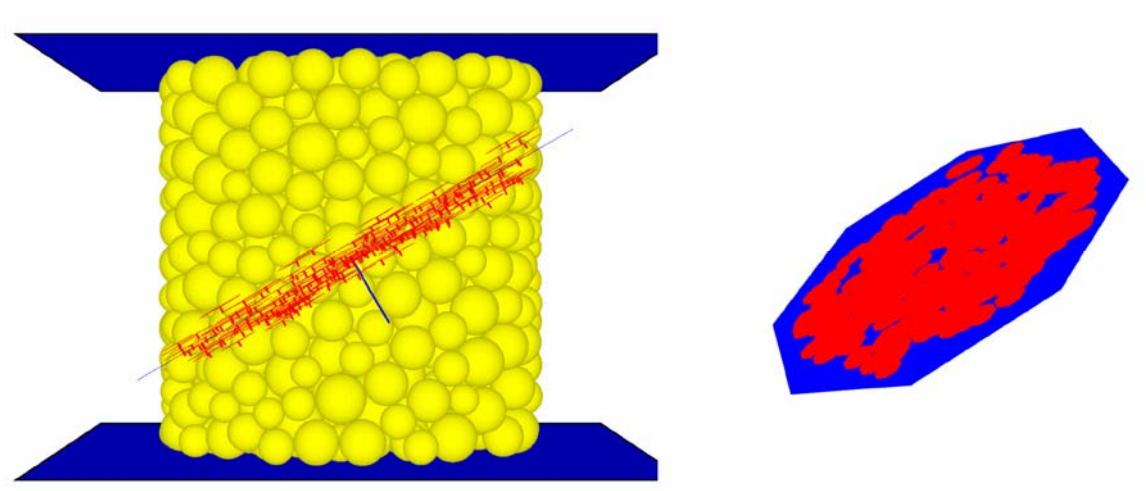

Figure 10 PFC3D specimen after insertion of joint (left: side view, right: rotated view showing macroscopic joint and 249 smooth-joint contacts

The joint properties are set to

$$\left(\bar{k}_n = \bar{k}_s\right) \cong \frac{E}{L} \cong \frac{E}{\tilde{D}} = \frac{70\times10^9 \ \text{N/m}^2}{3\times10^{-3} \ \text{m}} = 2.3\times10^{13} \ \text{N/m}^3$$

$$\bar{\lambda} = 1.0 \ \text{(set by } \texttt{sj\_Make}\text{)}$$

$$\mu = 0.5 \qquad (7)$$

$$\psi = 0$$

$$M = 0, \quad \sigma_c = \tau_c = 0.0 \ \text{(not bonded)}$$

where the stiffnesses per unit area are chosen to approximately equal the stiffnesses per unit area of a one-particle width slice of the bonded material. (The relation is derived by noting that stiffness equals AE/L, the macroscopic modulus of the Lac du Bonnet granite is 70 GPa and the average particle diameter is 3 mm.)

The first step of an unconfined-compression test requires that the specimen be seated by applying a small axial stress (defined by `mt_tas`). With an initial axial stress of –0.1 MPa and a joint friction coefficient of 0.5, the joint begins to slide during the seating process (see Figures 11 and 12). If the joint friction coefficient is increased to 1.0, then the seating is successful and a test can be performed.

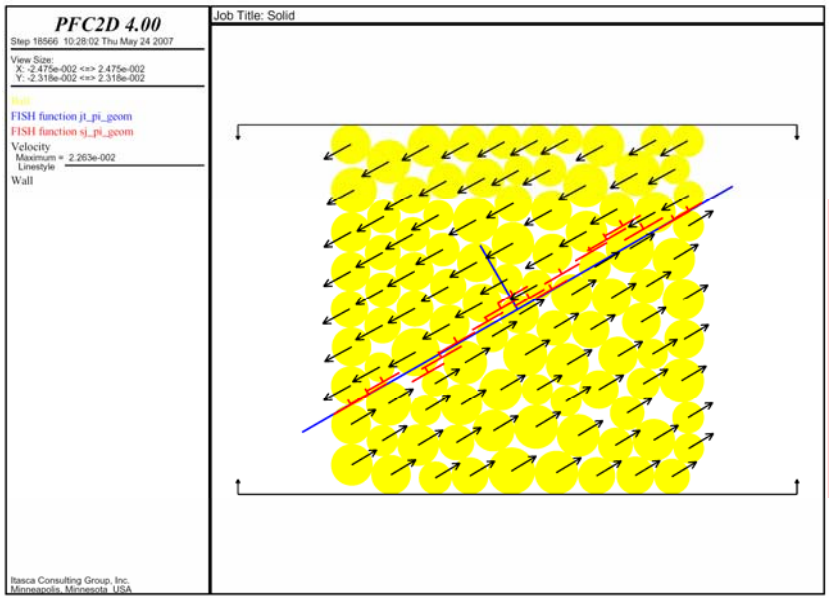

Figure 11 Velocity field while seating the PFC2D specimen (friction coefficient of 0.5) with an axial stress of –0.1 MPa (The specimen is failing by sliding along the joint.)

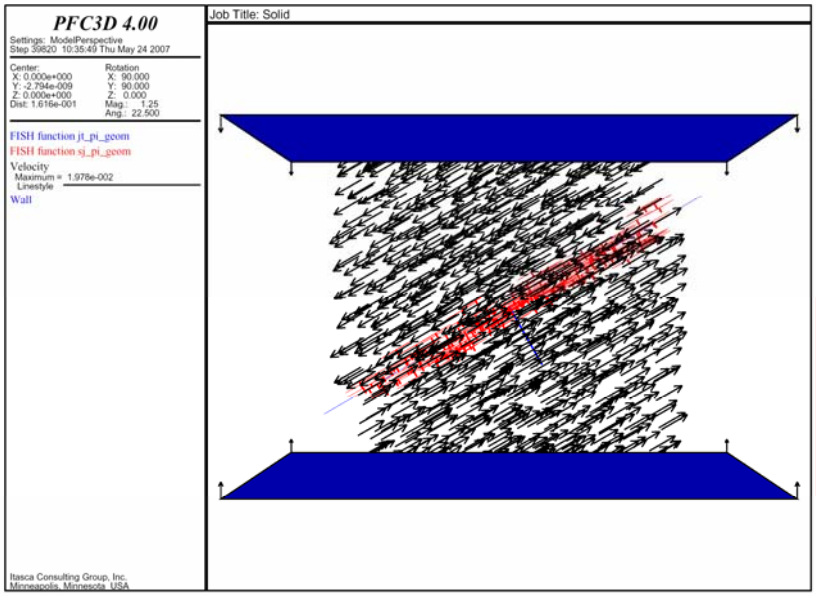

Figure 12 Velocity field while seating the PFC3D specimen (friction coefficient of 0.5) with an axial stress of –0.1 MPa (The specimen is failing by sliding along the joint.)

The second example (see the data files in the directories `fist\templates\LdB\2d\sj-2d` and `fist\templates\LdB\3d\sj-3d`, driven by `Solid2-sj.dvr`) adds seven through-going joints at a uniform spacing to a bonded-particle specimen, and then performs a compression test at 1.0 MPa confinement on the specimen. The bonded-particle model of Lac du Bonnet granite (described in the first example) with a resolution of approximately 20 particles across the specimen width is first created. Seven through-going joints at a 10-mm spacing and oriented with a –30 degree dip angle in the 2D model and a –60 degree dip angle and 0 degree dip direction in the 3D model are inserted. The joints are shown in Figures 13 and 14.

The joint properties are the same as those used in the first example, except that the friction coefficient is set to zero. The compression test reaches a steady-state axial stress of 1.8 MPa in the 2D model and 3.3 MPa in the 3D model. At this point, a mechanism has formed whereby upper and lower blocks are sliding (see Figures 15 and 16). Plots of contact forces (shown for the 2D case in Figure 17) confirm that no shear forces are acting on the joint planes.

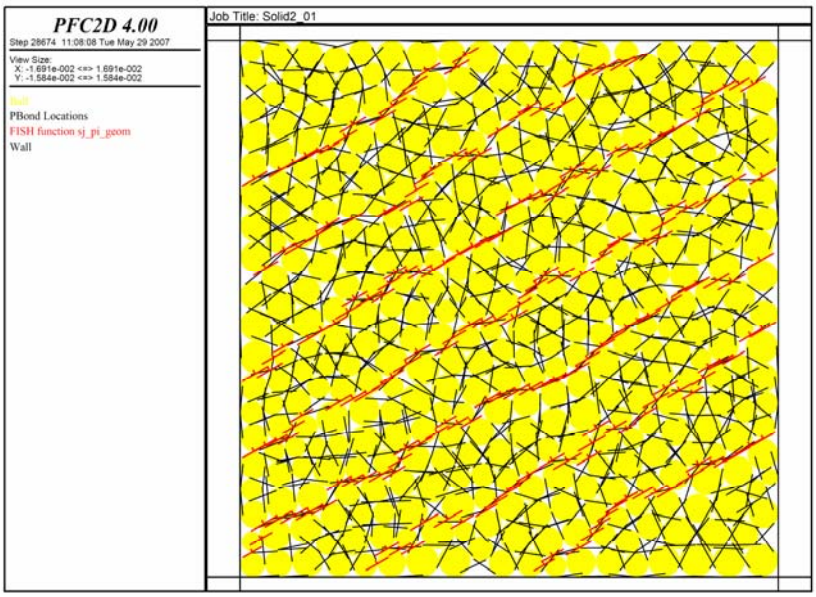

Figure 13 Particles, parallel bonds and seven joints in the PFC2D specimen (consisting of 204 smooth-joint contacts)

Figure 14 PFC3D specimen after insertion of the seven joints (consisting of 5419 smooth-joint contacts)

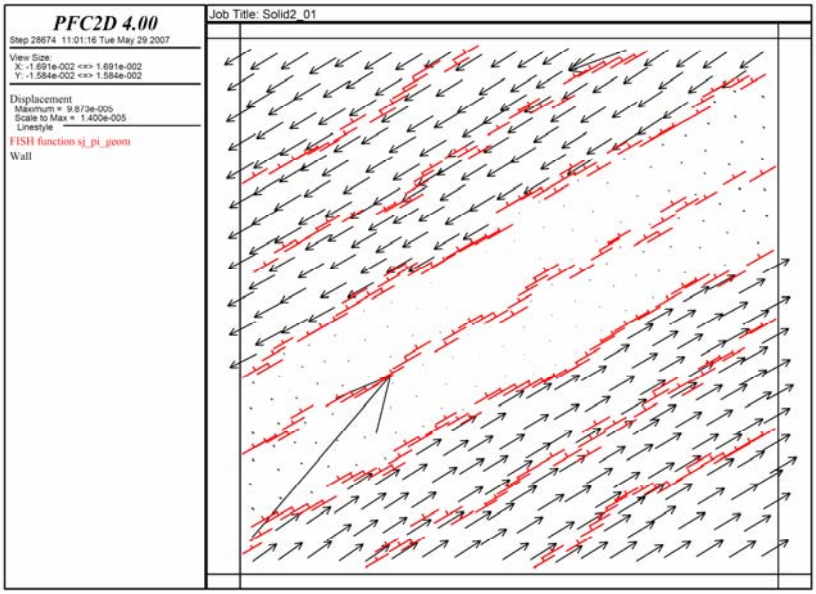

Figure 15 Displacement field in the PFC2D specimen at axial strain of 0.05%

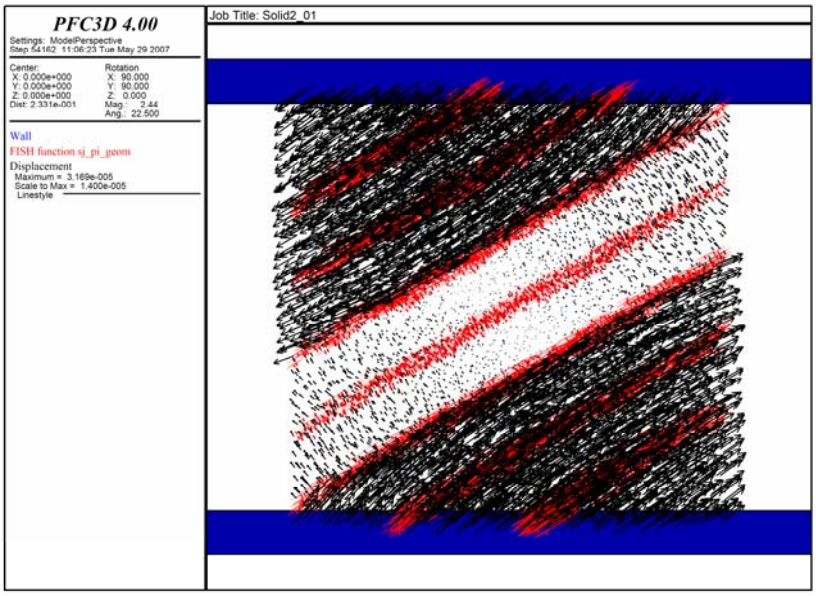

Figure 16 Displacement field in the PFC3D specimen at axial strain of 0.05%

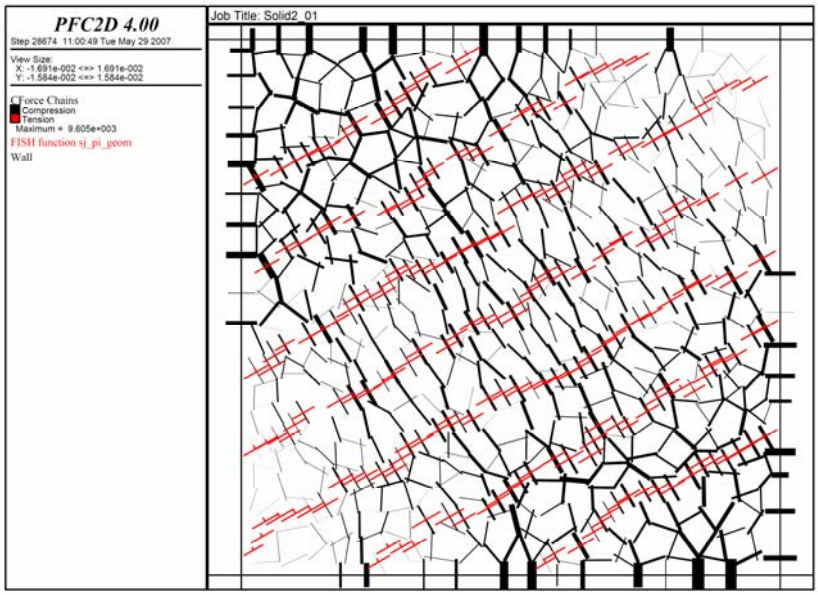

Figure 17 Contact forces in the PFC2D specimen at axial strain of 0.05%

2.4.4.4 Demonstration of smooth-joint contact logic

This example (see the data files in the directories `fist\templates\LdB\2d\sj-2d\LargeSlide` and `fist\templates\LdB\3d\sj-3d\LargeSlide`, driven by `LargeSlide.dvr`) demonstrates large sliding motion on a joint that is represented as a collection of smooth-joint contacts. A PFC2D rectangular and PFC3D cylindrical specimen is created, removed from the material vessel and allowed to expand. A through-going joint oriented at 30 degrees from the horizontal with a friction coefficient of one is created. The joint is represented by 19 and 56 smooth-joint contacts (given by `sj_num`) in the 2D and 3D models, respectively. A vertical wall is added to the left of the specimen to limit the lateral motion of the top block. The bottom layer of particles is fully fixed. Gravity is activated, and the system is allowed to reach static equilibrium. The blocks are stable for a joint friction coefficient of one. The joint friction coefficient is reduced to zero, and the top block begins to slide until it butts up against the left wall (see Figures 18 and 19). At this point, the 2D and 3D models contain 26 and 79 smooth-joint contacts, respectively. The new contacts were added by the function `sj_Add` (which is described in Section 2.2.4.2).

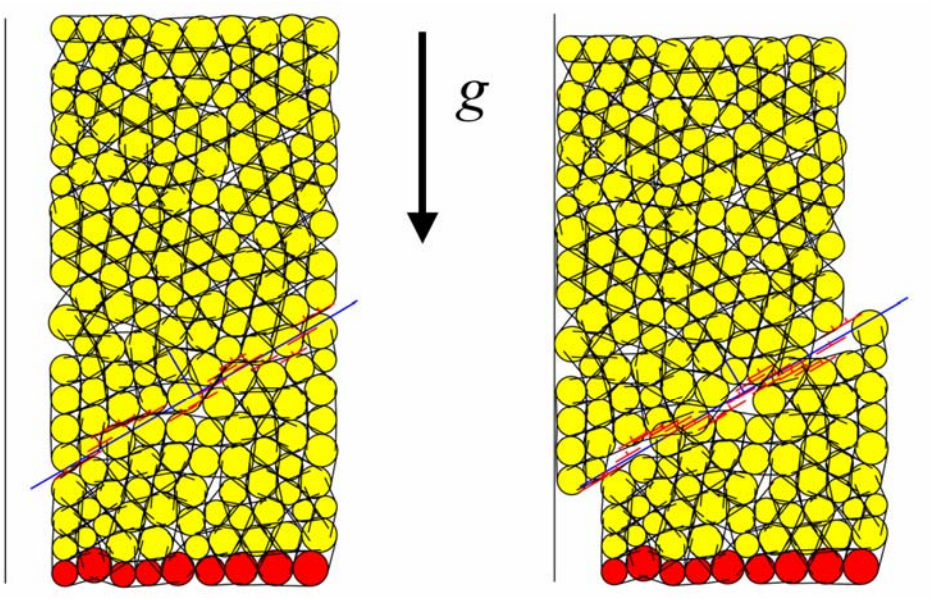

Figure 18 Stable PFC2D models with joint friction coefficients of 1.0 (left) and 0.0 (right)

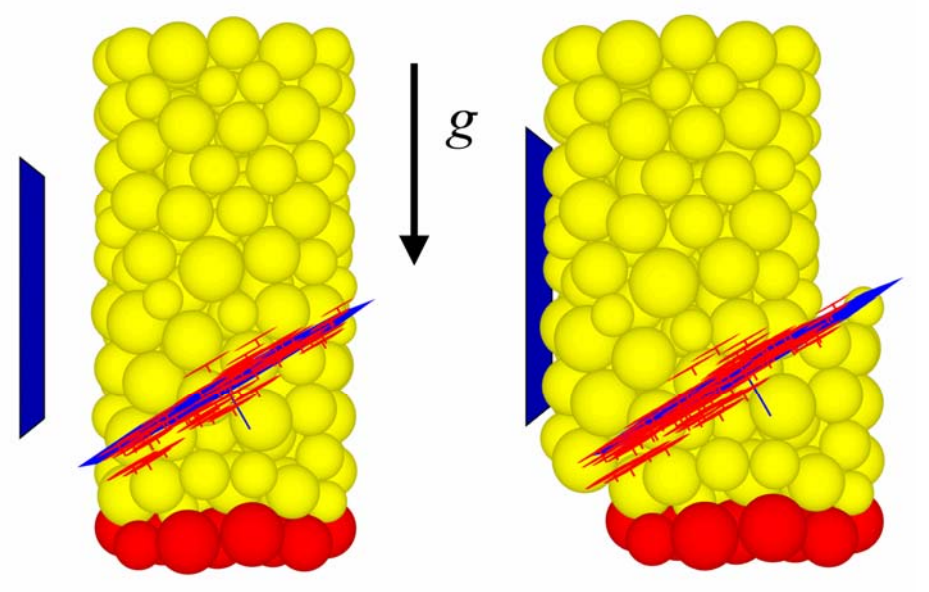

Figure 19 Stable PFC3D models with joint friction coefficients of 1.0 (left) and 0.0 (right)

2.4.4.5 Joint mechanical properties

The information in this section is taken from Itasca (2003), which should be consulted for more information.

There are well-established methods for the characterization of joint mechanical properties (Barton, 1976; Stephansson, 1985; Barton and Stephansson, 1990). Joint properties are conventionally derived from laboratory testing (e.g., triaxial, direct shear, or tilt tests). These tests can produce physical properties for joint friction angle, cohesion, dilation angle, and tensile strength, as well as joint normal and shear stiffnesses. The joint cohesion and friction angle correspond to the parameters in the Coulomb strength criterion.

Values for normal and shear stiffnesses for rock joints range from 10 to 100MPa/m, for joints with soft clay in-filling, to over 100 GPa/m, for tight joints in granite and basalt. Published data on stiffness properties for rock joints are limited; summaries of data can be found in Kulhawy (1975), Rosso (1976), and Bandis et al. (1983). Additional data has been generated by the various research programs for nuclear waste disposal. Most of this data can be obtained from the websites of the nuclear waste disposal management companies.

Published strength properties for joints are more readily available than stiffness properties. Summaries can be found, for example, in Jaeger and Cook (1969), Kulhawy (1975) and Barton (1976). Friction angles can vary from less than 10 degrees for smooth joints in weak rock, such as tuff, to over 50 degrees for rough joints in hard rock, such as granite. Joint cohesion can range from zero to values approaching the compressive strength of the surrounding rock.

Joint properties measured in the laboratory typically are not representative of those for real joints in the field (Pinto de Cunha, 1990). Scale dependence of joint properties is a major question in rock mechanics. Often, the only way to guide the choice of appropriate parameters is by comparison to similar joint properties derived from field tests; however, field test observations are extremely limited — some results are reported by Kulhawy (1975).

Approximate stiffness values can be back-calculated from information on the deformability and joint structure in the jointed rock mass and the deformability of the intact rock. If the jointed rock mass is assumed to have the same deformational response as an equivalent elastic continuum, then relations can be derived between jointed rock properties and equivalent continuum properties — see Itasca (2003).

Several expressions have been derived for two- and three-dimensional characterizations and multiple joint sets. References for these derivations can be found in Singh (1973), Gerrard (1982(a) and (b)), and Fossum (1985). Analytical solutions for estimating the equivalent properties of fractured rock masses are limited to simple fracture geometries (Salamon, 1968; Singh, 1973; Amadei and Goodman, 1981; Amadei, 1988).

There is a limit to the maximum joint stiffnesses ($\bar{k}_n$ and $\bar{k}_s$) that are reasonable to use in a PFC2D/3D model. If the physical normal and shear stiffnesses are less than ten times the equivalent stiffnesses of adjacent contacts, then there is no problem in using physical values. (The equivalent stiffness is the largest total stiffness per unit area of the contacts adjacent to the joint — e.g., the total stiffness per unit area of a parallel-bonded contact is equal to the parallel bond stiffness per unit area plus the contact stiffness divided by the contact area.) If the ratio is more than ten, the solution time will be significantly longer than for the case in which the ratio is limited to ten, without much change in the behavior of the system. Serious consideration should be given to reducing supplied values of joint normal and shear stiffnesses to improve solution efficiency. There may also be problems with particle interpenetration if the joint normal stiffness is very low. A rough estimate should be made of the joint normal displacement that would result from the application of typical stresses in the system ($u = \sigma / \bar{k}_n$). This displacement should be small compared to typical particle size. If it is greater than, say, 10% of an adjacent particle diameter, then either there is an error in one of the numbers or the stiffness should be increased.

REFERENCES

Amadei B and Goodman RE 1981. "A 3-D constitutive relation for fractured rock masses."In: Selvadurai APS (ed), Proc. Int. Symp. on the mechanical behavior of structured media, Ottawa, Part B, pp. 249-268.

Amadei B 1988. "Strength of a regularly jointed rock mass under biaxial and axisymetric loading conditions." Int. J. Rock Mech. Min. Sci. & Geomech. Abstr.;25:3-13.

Bandis et al. (1983) --- get from reference list of Chapter 3 of User's Guide volume of 3DEC 3.0 manual.

Barton N 1976. "The Shear Strength of Rock and Rock Joints." Int. J. Rock Mech. Min. Sci.;13:255-279.

Barton N and Stephansson O 1990. "Proceedings of the International Symposium on Rock Joints". 4-6 June, Loen, Norway. AA Balkema, Rotterdam.

Fossum AF 1985. "Effective elastic properties for a randomly jointed rock mass." Int. J. Rock. Mech. Min. Sci.;22:467-470.

Gerrard (1982(a) and (b)) --- get from reference list of Chapter 3 of User's Guide volume of 3DEC 3.0 manual.

Itasca Consulting Group, Inc. (2003) ***3DEC (3 Dimensional Distinct Element Code)***, Version 3.0, User's Guide volume, pp. 3-100 to 3-101.

Jaeger and Cook (1969) --- get from reference list of Chapter 3 of User's Guide volume of 3DEC 3.0 manual.

Kulhawy (1975) --- get from reference list of Chapter 3 of User's Guide volume of 3DEC 3.0 manual.

Pinto de Cunha, A (Ed.) 1990. "Scale effects in rock masses". A A Balkema, Rotterdam, pp.339.

Rosso (1976) --- get from reference list of Chapter 3 of User's Guide volume of 3DEC 3.0 manual.

Salamon MDG 1968. "Elastic moduli of a stratified rock mass." Int. J. Rock Mech. Min. Sci. & Geomech. Abstr.;5:519-527.

Singh B 1973. "Continuum characterization of jointed rock masses." Int. J. Rock Mech. Min. Sci. & Geomech. Abstr.;10:311-335.

Stephansson O (Ed.) 1985. "Proceedings of the International Symposium on Fundamentals of Rock Joints". 15-20 September, Björkliden, Sweden. Centek Publishers.